Using 2D and 3D Face Representations to Generate Comprehensive Facial Electromyography Intensity Maps*

Tim Büchner[1] [0000−0002−6879−552X], Sven Sickert[1] [0000−0002−7795−3905], Roland Graßme[2], Christoph Anders[2] [0000−0002−5580−5338], Orlando Guntinas-Lichius[3] [0000−0001−9671−0784], and Joachim Denzler[1] [0000−0002−3193−3300]

[1] Computer Vision Group, Friedrich Schiller University Jena, 07743 Jena, Germany
{tim.buechner,sven.sickert,joachim.denzler}@uni-jena.de

[2] Division of Motor Research, Pathophysiology and Biomechanics, Clinic for Trauma, Hand and Reconstructive Surgery, Jena University Hospital, 07747 Jena, Germany
{christoph.anders,roland.grassme}@med.uni-jena.de

[3] Dept. of Otorhinolaryngology, Jena University Hospital, 07747 Jena, Germany
{orlando.guntinas}@med.uni-jena.de

Abstract. Electromyography (EMG) is a method to measure muscle activity. Physicians also use EMG to study the function of facial muscles through intensity maps (IMs) to support diagnostics and research. However, many existing visualizations neglect anatomical structures and disregard the physical properties of EMG signals. The variance of facial structures between people complicates the generalization of IMs, which is crucial for their correct interpretation. In our work, we overcome these issues by introducing a pipeline to generate anatomically correct IMs for facial muscles. An IM generation algorithm based on a template model incorporates custom surface EMG schemes and combines them with a projection method to highlight the IMs on the patient's face in 2D and 3D. We evaluate the generated and projected IMs based on their correct projection quality for six base emotions on several subjects. These visualizations deepen the understanding of muscle activity areas and indicate that a holistic view of the face could be necessary to understand facial muscle activity. Medical experts can use our approach to study the function of facial muscles and to support diagnostics and therapy.

Keywords: Medical Visualization · EMG Intensity Maps · Projections · Emotion · Mimics · Facial Muscles

1 Introduction

Many medical imaging techniques utilize 2D or 3D visualizations to support decision-making during clinical routine and research. To gain insight into the

* Supported by Deutsche Forschungsgemeinschaft (DFG - German Research Foundation) project 427899908 BRIDGING THE GAP: MIMICS AND MUSCLES (DE 735/15-1 and GU 463/12-1).

function of the facial muscles, medical experts utilize electromyography (EMG) schemes applied to the face [11, 16]. Intensity maps (IMs) are a common way to display the spatial relations among muscles [11, 16, 19]. Given the complexity of the facial muscles and their 3D movement [7], IMs are a valuable tool for studying the function of facial muscles and support diagnostics and therapy. However, such visualizations often neglect the anatomical locations of surface electrodes, the physical properties of EMG signals, the interaction of individual facial muscles, and the individual's facial structure for highlighting.

We overcome these limitations by introducing a pipeline for anatomically correct facial muscle intensity maps. First, we use a canonical template face model as a base for the complex interwoven network of facial muscles [13, 18]. Based on this model, we support two standard EMG schemes and interpolate between surface electrodes incorporating the physical properties of EMG signals [11, 16]. Lastly, we project the IMs onto the patient's face in 2D and 3D to indicate muscular activity. Our projection algorithm considers the patients' facial head shape, pose, and expression. As a result, we give physicians a tool to study the facial muscles' functions projected onto the patient's face and support diagnostics and therapy by releasing our work as independent open source libraries[4].

2 Methods

The main limitations of current EMG IM visualizations are the lack of 3D anatomical information in general and the missing relations of individual facial structures, which is crucial for correct interpretation. First, we focus on generating anatomically correct IMs employing a canonical face template model [13]. We demonstrate the process using two standardized EMG schemes [11,16]. However, our method is not limited to these schemes and is extendable to custom mappings to enable specialized research. Projecting the generated IMs onto the patient's face highlights the muscular activity in a 2D image or 3D face model.

2.1 EMG Intensity Map Generation

By definition, muscle activity is the electrical response of the muscle cells under load measured in volts [22]. The acquired time series of the electrical response is called an electromyogram (EMG). Experts visualize the spatial relations using intensity maps (IMs) based on a planar grid structure neglecting anatomical placement and three-dimensionality of the muscles and their movements (see Figure 1) [16]. However, electrode placement is crucial for interpolation as the EMG signal drops off quadratically with distance [22]. Furthermore, a categorical colormap implies that large areas around the electrodes have the same intensity intervals, which conflicts with the EMG's physical properties.

We propose to circumvent these limitations by explicitly considering: anatomical electrode locations, an interpolation comprising correct physical properties,

[4] www.github.com/cvjena/electromyogram, www.github.com/cvjena/face-projection

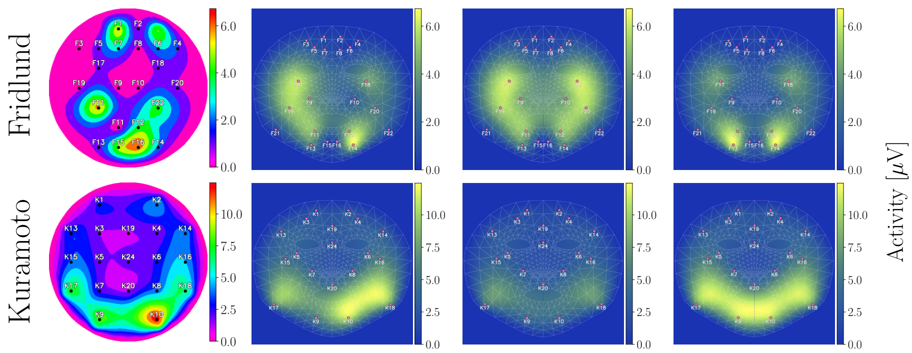

(a) Conventional **(b) Ours** (c) Mirror Right (d) Mirror Left

Fig. 1: Displaying the intensity maps for a smiling expression for two different EMG schemes (Fridlund scheme, upper row; Kuramoto scheme, lower row): The first column shows the conventional approach neglecting anatomical structures, and the second column shows the proposed intensity maps. The third and fourth column shows the lateral mirrored maps focusing on the face's left and right sides.

and a continuous colormap [5]. First, we define the anatomical electrode locations based on the facial structure inside the canonical face model [13]. Such an approach offers several advantages: (i) The template model ensures a patient-independent visualization, which is crucial for interpolation. (ii) Semantic facial landmarks ensure proper electrode location definition, and (iii) we can utilize existing models for correct facial landmark detection for the projections [18].

The canonical face model contains 468 facial landmarks [13], which we use to determine the electrode locations in a planar view. We define the electrode locations for two standardized facial EMG schemes, Fridlund [11] and Kuramoto [16], which we compare in our evaluation. Figure 2 displays the anatomical and corresponding locations on the canonical face model. Additionally, the warped view helps to comprehend the spatial connections among the electrodes and the facial landmarks. The blue dots mark the electrode locations, and the green squares depict the hull boundary of the face model.

These electrode locations are crucial for approximating the EMG signal's spatial properties via interpolation in the next step. Points of the outer hull form an interpolation boundary and act as electrodes without muscle activity, having an amplitude of 0 V. We deploy radial basis function (RBF) interpolation to approximate the EMGs' spatial properties inside the canonical face model [9,28]. Specifically, a thin plate spline as a kernel function in the form of $r^2 \cdot \log r$ models the signal drop off [28], with r being the distance of each location to the center point. As we ensured correct anatomical placement beforehand, the electrode values can be interpolated without weights ensuring a valid spatial behavior approximation of the EMG signal between the electrodes.

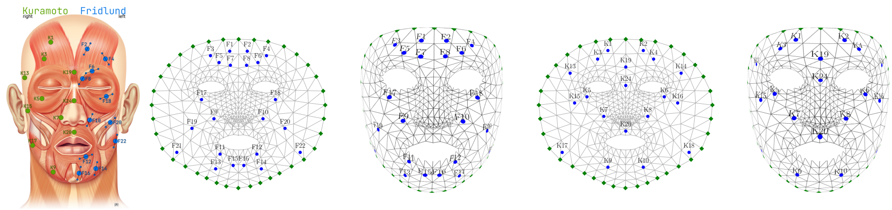

(a) Anatomical locations (b) Fridlund planar view (c) Fridlund warped view (d) Kuramoto planar view (e) Kuramoto warped view

Fig. 2: The anatomical electrode locations of the Fridlund (blue) [11] and Kuramoto (green) [16] schemes are shown in (a). The matching locations (blue) on the canonical face are shown as planar and warped views in (b, c) and (d, e).

Visualizing unilateral muscle activity is highly relevant for some medical diseases, such as unilateral facial palsy [26]. In this case, the muscle activity is not symmetric due to muscle inactivity or hypoactivity on the palsy side, compensatory hyperactivity of the contralateral side, or both combined. We can mitigate interpolation artifacts by laterally mirroring along the midline of the face model and interpolating each side separately. Thus, we enforce a symmetric interpolation of the face sides and remove contralateral artifacts, giving insight into the unilateral muscle activity. In Figure 1, we visually compare the conventional approach [16] with our proposed method. We show the IMs of a smiling expression and use a sequential colormap (*Imola*) to visualize the continuous data [5]. 2D grid interpolation neglects the anatomical electrode locations and gives the impression of discrete areas of muscle activity, resulting in a distorted visualization. The connection between electrode locations and interpolated values is not apparent and might hinder the interpretation of the IMs. However, both approaches still capture the properties of the EMG schemes, as Fridlund specializes in specific muscles, while Kuramoto is better for muscle activity regions [19].

2.2 Anatomical 2D Face Projection

We have seen in the previous section that interpolating the EMG signal's spatial properties is crucial for the IMs' quality. However, the IMs are still 2D visualizations of the spatial relations between muscle activations without a patient's facial structure. We propose further enhancing the generated IMs' quality by projecting them onto the face while preserving anatomical properties. This step enhances muscle activity visualization, improving the IMs' interpretability.

One of the main advantages of the canonical face model is that we can deploy existing facial landmark detection algorithms [18]. Thus, we can avoid fine-tuning our data and ensure general visualization capabilities. Using the same 468 facial landmarks allows us to generate a one-to-one mapping between the IMs and the face[5]. However, during the acquisition of the EMG signals, the face is covered

[5] All shown individuals agreed to have their images published in terms with the GDPR

(a) Cables and electrodes (b) Projected Fridlund IMs (c) Head rotation invariant (d) Avoiding depth clipping

Fig. 3: We show the projection of the IMs onto the face model. In (a), the face is covered in cables and electrodes while acquiring the EMG signals. The restored facial features with the overlaid muscle activity are shown in (b). Figures (c) and (d) depict head rotation invariance and the prevention of depth clipping.

in cables and electrodes, as shown in Figure 3a. Hence, many facial features are obstructed, and existing algorithms cannot detect them. We follow the work of [3] and restore the original facial features, which visually improves the overlaid muscle activity, as shown in Figure 3b.

As the interpolation approximates the EMG signal's spatial relations over the entire template model, areas without muscle activity also have interpolated values, including the eyes, mouth, and lips; see Figure 1a. However, we remove these areas for a more natural and intuitive impression of the face and muscle activity by masking them out in the IMs. A consequence of deleting the areas of the eyes and mouth is that the triangulation of the canonical face model is no longer valid. Therefore, a newly calculated triangulation maps the template model to the face [15, 24], depicted in Figure 4. We obtain corresponding pairs $(T^{(i)}_{\text{face}}, T^{(i)}_{\text{IM}})$ for each triangle $T^{(i)}$ in the triangulation to compute the projection.

First, we extract the bounding boxes for each triangle pair, from which we compute the affine homomorphism described by the matrix $M \in \mathbb{R}^{3\times3}$. Each pixel in the triangle $T^{(i)}_{IM}$ is then mapped to the corresponding pixel in the triangle $T^{(i)}_{face}$ using M. Bicubic interpolation approximates intermediate pixel values as the projection might contain different scales between the IM and the face. Additionally, the projection algorithm discards pixels outside the triangle to ensure a valid projection without overlap. As face parts might not be visible during head rotation, shown in Figure 3c, depth clipping artifacts might occur. We circumvent this issue by sorting the triangles from back to front using the estimated depth values of each triangle [18]. Please note the default resolution for IMs is 1024×1024 pixels, while the face images have a resolution of 256×256 pixels. Thus, we obtain a highly detailed projection with electrode locations and the interpolated values blended onto the face, as shown in Figure 3b.

Since our projection solely depends on facial landmarks, we can project the IMs onto any face [18]. Furthermore, our approach is independent of the facial pose and rotation, as shown in Figure 3c. This advantage allows our method to

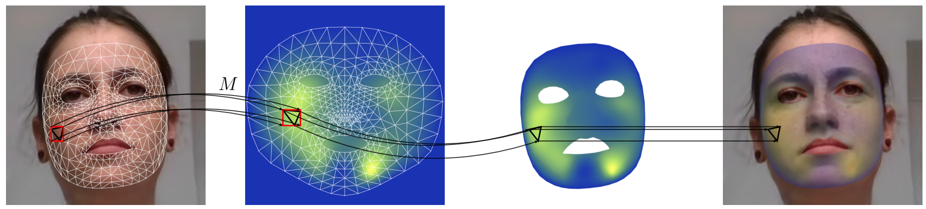

(a) Triangle $T^{(i)}_{face}$ on the face

(b) Matching triangle $T^{(i)}_{IM}$ on the intensity map

(c) Affine transformation of triangle $T^{(i)}_{IM}$ onto the face

(d) Blending onto the face with opacity

Fig. 4: Triangle correspondence between the face and the IM: We compute the affine matrix M between the bounding boxes (red) of $T^{(i)}_{\text{IM}}$ and $T^{(i)}_{\text{face}}$. Each pixel of the IM is transformed to the corresponding pixel in the face using M.

be used on static images and videos, opening up the research of dynamic analysis of muscle activity. The combination of interpolation and projection allows us to visualize muscle activity more intuitively for medical professionals and patients.

2.3 Anatomical 3D Face Projection

Leveraging the 3D structure of the face will further enhance the interpretability of muscle activity. Such a step would enable visualization in a virtual reality environment or with holographic displays[6]. To achieve this, we utilize the resulting 2D projection as the basis for the 3D transformation. As this projection already ensures the anatomical correctness of the muscle activity, the 3D representation is also anatomically correct. We present two 3D model generation approaches based on depth sensors and monocular depth estimation models, respectively.

Our first approach operates on depth maps provided by cameras such as the Intel RealSense D435. Given the RGBD data and the intrinsic camera parameters, the computed point cloud describes the 3D face structure. However, replacing the RGB image with the projected 2D intensity map only changes the vertex color of the point cloud. To obtain a mesh representation of the face, we use Poisson surface reconstruction [14]. Reconstructed areas with lower confidence than 0.03 are removed, and only the largest connected component is kept. Lastly, using Laplacian smoothing along the z-axis ensures that the face's surface is smooth and contains no artifacts from the depth sensor [25,27]. We show the resulting mesh from the depth sensor in Figure 5a.

Our second approach utilizes monocular depth estimation models to obtain a 3D representation of the face. Hence, it does not require a depth sensor and can be retrospectively employed on existing images and videos. Such monocular

[6] We support LookingGlass Portrait (Looking Glass Factory Inc., New York, USA) natively in our pipeline.

(a) Depth sensor projection (b) Projection with 3DDFA [29] (c) Projection with DECA [10]

Fig. 5: We display three different 3D reconstruction variants with projected intensity maps. They include a head scan reconstruction (a), the monocular depth model *3DDFA* (b) [29], and the 3D morphable model *DECA* (c) [10].

models are trained on large data sets of facial images with corresponding 3D scans to approximate the underlying facial structure. Given an RGB image, the 3DDFA model [12, 29] estimates the Basel Face Model [20] to obtain a 3D mesh of only the face. The DECA model [10] predicts the FLAME model [21], which includes the head, neck, and upper torso. They are not accurate compared to a 3D scan, and significant deviations occur due to the underlying template model assumptions, as is visible in Figure 5b and Figure 5c. However, they are sufficient for visualizing muscle activity on a 3D face.

3 Data Acquisition

Our dataset combines synchronous surface EMG and RGBD data recording for healthy probands. We use an Intel RealSense D435 camera with a 1280×720 pixels resolution and a frame rate of 30 fps. All probands are seated in front of the camera at eye level with a distance of 1.0 meters to ensure the face is visible in the depth sensor's field of view. Our surface EMG measurements follow the work of Mueller et al. [19], merging doubled electrodes for Fridlund and Kuramoto [11, 16]. Each proband has 62 surface electrodes attached while mimicking voluntary facial expressions instructed by a video tutorial [23].

Our probands are recorded with and without applied surface electrodes to restore the facial expression using CycleGANs [3]. Otherwise, existing landmark detection methods would fail and result in incorrect projections. The restored facial expressions are used for the projection in all visualizations, as shown in Figure 3b. The processing of the EMG data follows the guidelines discussed in [11, 16, 19]. The muscle activity is measured with 4096 samples per second. We normalize each channel's average to zero and remove power line noise with a notch filter at 50 Hz. Furthermore, we apply an FIR band-pass filter in this

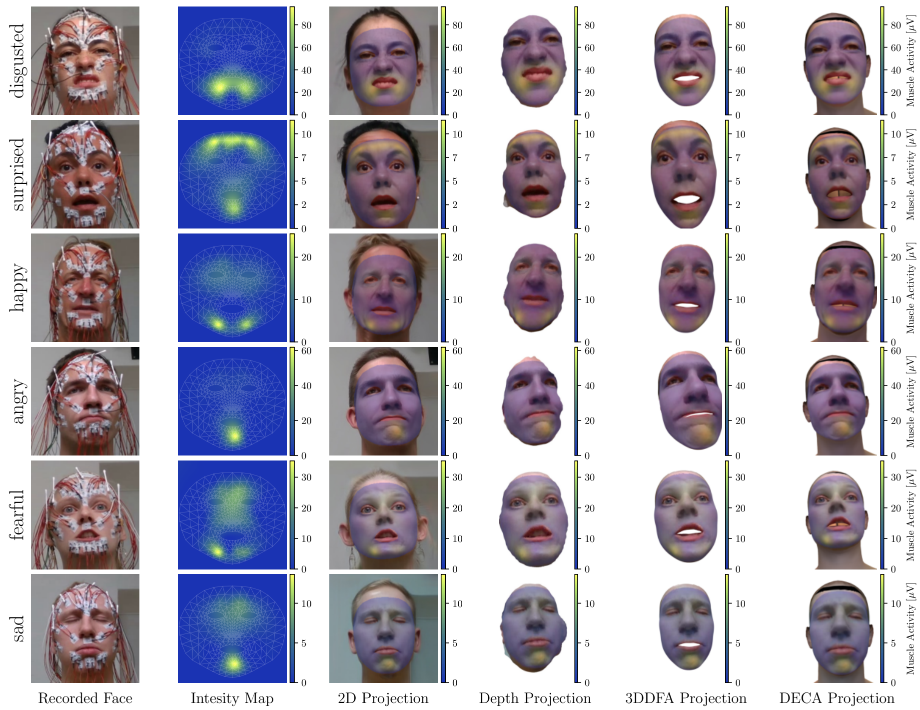

Fig. 6: Muscle activity patterns for the base emotions [6] using Fridlund [11] scheme: We show the original facial expression with the attached surface electrodes, the generated corresponding intensity maps (IMs), and projection onto the restored facial expression [3]. The Fridlund scheme visualizes individual muscle activity during expressions. (Best viewed digitally.)

range because most muscle activity ranges from 10 to 500 Hz [11]. Lastly, we compute the root mean square with a 128 ms sliding window to match video frames and EMG data. Thus, data is synchronous with an error of up to 8 ms.

4 Evaluation

Our evaluation focuses on the visual quality and the possible insights gained from the generated intensity maps of the resulting muscle activity patterns for the six base emotions [6]. We do not assess the muscle activity patterns' correctness regarding the defined facial action coding system [7], as this is not the focus of our work and is still disputed [1,8]. However, our method allows medical professionals to evaluate the correctness of the muscle activity patterns in future research. We measure with the Fridlund [11] and Kuramoto [16] schemes jointly during the recording but evaluate them separately to avoid visual interference. The resulting muscle activity patterns are shown in Figure 6 and Figure 7 for

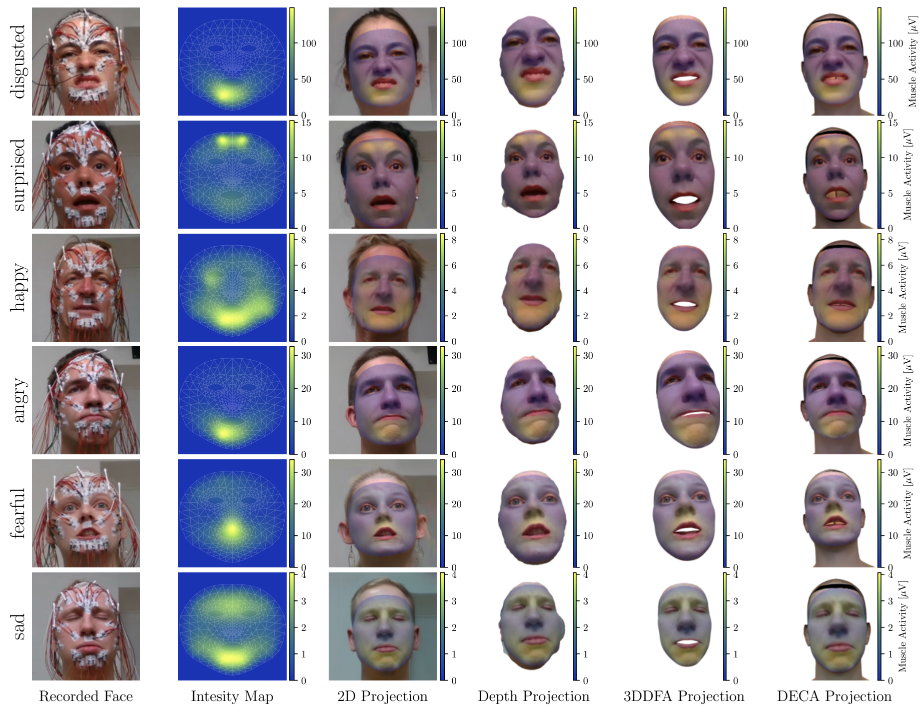

Fig. 7: Muscle activity patterns for the base emotions [6] using Kuramoto [16] scheme: We show the original facial expression with the attached surface electrodes, the generated corresponding intensity maps (IMs), and projection onto the restored facial expression [3]. The Kuramoto scheme visualizes the muscle activity areas during expressions. (Best viewed digitally.)

six different probands varying in gender and age. Please note that we do not normalize amplitudes between the emotions as they can contribute to their differentiation, as visible in Figure 6 for `sad` and `angry`. Furthermore, we refrain from adding the label locations to the visualizations to avoid visual clutter and instead refer to the electrode locations in Figure 2. For the Fridlund scheme, we observe that mainly single muscles are dominating, as expected [7], but also that other facial areas are involved to a lesser extent. This observation could indicate that the interwoven network of facial muscles is more active during facial expressions than previously thought [1,2,4]. The overall facial activations are even more visible with the Kuramoto scheme, highlighting the importance of a more holistic view of the facial muscles' activity. Combining both schemes' advantages could benefit future work to understand the facial muscles' activity better.

Our 2D IM projection algorithm works for different head shapes, orientations, expressions, and probands, as visible in Figure 6 and Figure 7. Comparing the surface electrode locations with the highlighted areas in the face, they largely overlap and thus confirm the correctness of our method. As we remove eye and mouth areas from the IMs, the mouth opening for `surprised` and eye closing for `sad` are not overlaid. Hence, our work allows for an individual analysis of the muscle activity patterns for each proband, not only for a generic face model.

The 3D visualizations differ considerably between the probands and methods, respectively. Only the depth sensor-based approach correctly captures the proband's original head shape, whereas the monocular methods strongly resemble the underlying template model. The projected IMs might lose some information due to underlying model biases during the computation, as visible for `happy` in Figure 7 where the mouth is *not open* but predicted *open* by the model. However, the monocular methods are still helpful for visualizing muscle activity patterns in 3D space, given that no depth sensor is available.

5 Conclusion

The proposed visualization methodology allows for an individualized analysis of muscle activity patterns by projecting the intensity maps onto the face's surface in 2D and 3D. This is a significant step from a generic face model and can help clinicians and researchers understand the variations in emotional expressions between individuals and patients, including those of different genders and ages. Our method is not limited to a specific head shape, orientation, or expression, as visible in Figure 6 and Figure 7.

Evaluation of these maps can provide insights into how multiple muscles and facial areas contribute to a particular emotional expression. Understanding the subtleties of facial muscle activation can be extremely useful for diagnosing patients with facial diseases in biofeedback and facial rehabilitation. For patients recovering from conditions like Bell's palsy or stroke that often affect facial muscles [17, 26], these visualizations could help therapists track recovery progress and plan individualized rehabilitation programs. Knowledge gained from understanding the subtle use of facial muscles can be applied in additional fields, like psychophysical experiments in psychology, acting, animation, advertising, etc., to make non-verbal communication appear more authentic and impactful.

Our evaluation results indicate that the muscle activity patterns are not as simple as previously postulated [1, 7]. The detailed results and comprehensive visual representations illustrated in this study establish a solid foundation for further investigation in the field. There is still ongoing dispute on facial expressions and muscles, and having such concrete visualizations and analysis could potentially aid in resolving these issues. A more holistic view of the facial muscles' activity seems to be necessary to understand the underlying processes better. The results and visualizations of this research can aid psychologists in studying and interpreting human emotions more accurately, thus enriching the science of understanding human behavior. The novelty of this approach lies not only in the specific techniques used but also in the fresh perspective it offers into the simultaneous mapping of muscle activations with corresponding facial expressions by bridging the gap between mimics and muscles.

References

1. Barrett, L.F., Adolphs, R., Marsella, S., Martinez, A.M., Pollak, S.D.: Emotional Expressions Reconsidered: Challenges to Inferring Emotion From Human Facial Movements. Psychological Science in the Public Interest **20**(1), 1–68 (Jul 2019). https://doi.org/10.1177/1529100619832930
2. Benitez-Quiroz, C.F., Srinivasan, R., Martinez, A.M.: Facial color is an efficient mechanism to visually transmit emotion. Proceedings of the National Academy of Sciences **115**(14), 3581–3586 (Apr 2018). https://doi.org/10.1073/pnas.1716084115
3. Büchner, T., Sickert, S., Volk, G.F., Anders, C., Guntinas-Lichius, O., Denzler, J.: Let's get the FACS straight - reconstructing obstructed facial features. In: International Conference on Computer Vision Theory and Applications (VISAPP). pp. 727–736. SciTePress (2023). https://doi.org/10.5220/0011619900003417
4. Cowen, A., Sauter, D., Tracy, J.L., Keltner, D.: Mapping the Passions: Toward a High-Dimensional Taxonomy of Emotional Experience and Expression. Psychological Science in the Public Interest **20**(1), 69–90 (Jul 2019). https://doi.org/10.1177/1529100619850176
5. Dasgupta, A., Poco, J., Rogowitz, B., Han, K., Bertini, E., Silva, C.T.: The Effect of Color Scales on Climate Scientists' Objective and Subjective Performance in Spatial Data Analysis Tasks. IEEE transactions on visualization and computer graphics **26**(3), 1577–1591 (Mar 2020). https://doi.org/10.1109/TVCG.2018.2876539
6. Ekman, P.: An argument for basic emotions. Cognition & emotion **6**(3-4), 169–200 (1992). https://doi.org/10.1080/02699939208411068
7. Ekman, P., Friesen, W.: Facial Action Coding System: A Technique for the Measurement of Facial Movement. Palo Alto: Consulting Psychologists Press (1978). https://doi.org/10.1037/t27734-000
8. Elfenbein, H.A., Ambady, N.: On the universality and cultural specificity of emotion recognition: A meta-analysis. Psychological Bulletin **128**(2), 203–235 (2002). https://doi.org/10.1037/0033-2909.128.2.203
9. Fasshauer, G.E.: Meshfree Approximation Methods with Matlab: (With CD-ROM), Interdisciplinary Mathematical Sciences, vol. 6. WORLD SCIENTIFIC (Apr 2007). https://doi.org/10.1142/6437
10. Feng, Y., Feng, H., Black, M.J., Bolkart, T.: Learning an animatable detailed 3D face model from in-the-wild images. ACM Transactions on Graphics **40**(4), 1–13 (Aug 2021). https://doi.org/10.1145/3450626.3459936
11. Fridlund, A.J., Cacioppo, J.T.: Guidelines for human electromyographic research. Psychophysiology **23**(5), 567–589 (Sep 1986). https://doi.org/10.1111/j.1469-8986.1986.tb00676.x
12. Guo, J., Zhu, X., Yang, Y., Yang, F., Lei, Z., Li, S.Z.: Towards fast, accurate and stable 3D dense face alignment. In: Proceedings of the European Conference on Computer Vision (ECCV) (2020)
13. Kartynnik, Y., Ablavatski, A., Grishchenko, I., Grundmann, M.: Real-time Facial Surface Geometry from Monocular Video on Mobile GPUs. arXiv:1907.06724 [cs] (Jul 2019)
14. Kazhdan, M., Bolitho, M., Hoppe, H.: Poisson Surface Reconstruction. The Eurographics Association (2006). https://doi.org/10.2312/SGP/SGP06/061-070
15. Kloeckner, A., Brun, L., Liu, B., Klemenc, S., Fkikl, A., Gohlke, C., Coon, E., Oxberry, G., Veselý, J., Wala, M., Smith, M., Potrowl, P., Kurtz, A.: MeshPy (Nov 2022). https://doi.org/10.5281/zenodo.7296572

16. Kuramoto, E., Yoshinaga, S., Nakao, H., Nemoto, S., Ishida, Y.: Characteristics of facial muscle activity during voluntary facial expressions: Imaging analysis of facial expressions based on myogenic potential data. Neuropsychopharmacology Reports **39**(3), 183–193 (Sep 2019). https://doi.org/10.1002/npr2.12059
17. Loyo, M., McReynold, M., Mace, J.C., Cameron, M.: Protocol for randomized controlled trial of electric stimulation with high-volt twin peak versus placebo for facial functional recovery from acute Bell's palsy in patients with poor prognostic factors. Journal of Rehabilitation and Assistive Technologies Engineering **7**, 2055668320964142 (Dec 2020). https://doi.org/10.1177/2055668320964142
18. Lugaresi, C., Tang, J., Nash, H., McClanahan, C., Uboweja, E., Hays, M., Zhang, F., Chang, C.L., Yong, M.G., Lee, J., Chang, W.T., Hua, W., Georg, M., Grundmann, M.: MediaPipe: A Framework for Building Perception Pipelines (Jun 2019). https://doi.org/10.48550/arXiv.1906.08172
19. Mueller, N., Trentzsch, V., Grassme, R., Guntinas-Lichius, O., Volk, G.F., Anders, C.: High-resolution surface electromyographic activities of facial muscles during mimic movements in healthy adults: A prospective observational study. Frontiers in Human Neuroscience **16** (2022). https://doi.org/10.3389/fnhum.2022.1029415
20. Paysan, P., Knothe, R., Amberg, B., Romdhani, S., Vetter, T.: A 3D Face Model for Pose and Illumination Invariant Face Recognition. In: 2009 Sixth IEEE International Conference on Advanced Video and Signal Based Surveillance. pp. 296–301. IEEE, Genova, Italy (Sep 2009). https://doi.org/10.1109/AVSS.2009.58
21. Ranjan, A., Bolkart, T., Sanyal, S., Black, M.J.: Generating 3D Faces Using Convolutional Mesh Autoencoders. In: Ferrari, V., Hebert, M., Sminchisescu, C., Weiss, Y. (eds.) Computer Vision – ECCV 2018, vol. 11207, pp. 725–741. Springer International Publishing, Cham (2018). https://doi.org/10.1007/978-3-030-01219-9_43
22. Robertson, D.G.E., Caldwell, G.E., Hamill, J., Kamen, G., Whittlesey, S.N.: Research Methods in Biomechanics. Human Kinetics, Champaign, Illinois, second edition edn. (2014)
23. Schaede, R.A., Volk, G.F., Modersohn, L., Barth, J.M., Denzler, J., Guntinas-Lichius, O.: Video Instruction for Synchronous Video Recording of Mimic Movement of Patients with Facial Palsy. Laryngo- rhino- otologie **96**(12), 844–849 (Dec 2017). https://doi.org/10.1055/s-0043-101699
24. Shewchuk, J.R.: Triangle: Engineering a 2D Quality Mesh Generator and Delaunay Triangulator. In: Lin, M.C., Manocha, D. (eds.) Applied Computational Geometry: Towards Geometric Engineering, Lecture Notes in Computer Science, vol. 1148, pp. 203–222. Springer-Verlag (May 1996)
25. Taubin, G.: Curve and surface smoothing without shrinkage. In: Proceedings of IEEE International Conference on Computer Vision. pp. 852–857 (Jun 1995). https://doi.org/10.1109/ICCV.1995.466848
26. Volk, G.F., Leier, C., Guntinas-lichius, O.: Correlation between electromyography and quantitative ultrasonography of facial muscles in patients with facial palsy. Muscle & Nerve **53**(5), 755–761 (2016)
27. Vollmer, J., Mencl, R., Müller, H.: Improved Laplacian Smoothing of Noisy Surface Meshes. Computer Graphics Forum **18**(3), 131–138 (1999). https://doi.org/10.1111/1467-8659.00334
28. Wahba, G.: Spline Models for Observational Data. CBMS-NSF Regional Conference Series in Applied Mathematics, Society for Industrial and Applied Mathematics (Jan 1990). https://doi.org/10.1137/1.9781611970128
29. Zhu, X., Liu, X., Lei, Z., Li, S.Z.: Face alignment in full pose range: A 3d total solution. IEEE transactions on pattern analysis and machine intelligence (2017)